

# Low-Temperature Epitaxy of Compressively Strained Silicon Directly on Silicon Substrates

D. SHAHRJERDI,<sup>1,2</sup> B. HEKMATSHOAR,<sup>1</sup> S.W. BEDELL,<sup>1</sup>  
M. HOPSTAKEN,<sup>1</sup> and D.K. SADANA<sup>1</sup>

1.—IBM T. J. Watson Research Center, Yorktown Heights, NY 10598, USA. 2.—e-mail: davood@us.ibm.com

We report epitaxial growth of compressively strained silicon directly on (100) silicon substrates by plasma-enhanced chemical vapor deposition. The silicon epitaxy was performed in a silane and hydrogen gas mixture at temperatures as low as 150°C. We investigate the effect of hydrogen dilution during the silicon epitaxy on the strain level by high-resolution x-ray diffraction. Additionally, triple-axis x-ray reciprocal-space mapping of the samples indicates that (i) the epitaxial layers are fully strained and (ii) the strain is graded. Secondary-ion mass spectrometry depth profiling reveals the correlation between the strain gradient and the hydrogen concentration profile within the epitaxial layers. Furthermore, heavily phosphorus-doped layers with an electrically active doping concentration of  $\sim 2 \times 10^{20} \text{ cm}^{-3}$  were obtained at such low growth temperatures.

**Key words:** Low temperature, epitaxial growth, compressive strain, heavily doped

Low-temperature epitaxy (LTE) of silicon has always been of particular interest for advanced silicon technology. The addition of strain engineering by LTE has the potential for numerous applications in the mainstream microelectronics industry. For example, LTE of strained Si can be utilized for carrier mobility enhancement in deeply scaled metal–oxide–semiconductor field-effect transistors. Additionally, LTE of heavily doped Si opens up the possibility for many applications with stringent thermal budget requirements such as forming the emitter for c-Si-based photovoltaic solar cells and growing raised source/drain for transistors fabricated on extremely thin silicon on insulator (ETSOI) substrates.

LTE of silicon has been reported earlier using molecular-beam epitaxy (MBE),<sup>1</sup> and plasma-enhanced chemical vapor deposition (PECVD).<sup>2–5</sup> The previous reports using PECVD technique have primarily examined the effect of the hydrogen dilution ratio ( $\text{HDR} = [\text{H}_2]/[\text{SiH}_4]$ ) and the growth temperature on the crystalline quality of the low-tempera-

ture epitaxial Si (epi-Si) and the critical thickness before the occurrence of the growth transition from crystalline to amorphous.

It should be realized that there is no known method to obtain biaxially compressive Si layers. Therefore, Ge atoms are epitaxially incorporated into the Si lattice structure to achieve compressive biaxial strain in Si.<sup>6</sup> However, uniaxial compressive strain can be locally applied to Si using the embedded silicon-germanium (e-SiGe) technique.<sup>7,8</sup> It is important to mention that growth of compressively strained  $\text{Si}_x\text{Ge}_{1-x}$  layers is typically performed at temperatures  $> 600^\circ\text{C}$ , for Ge mole fractions  $< 35\%$ . In this work, we report a unique epitaxial process that provides biaxial compressive strain directly on (100) silicon at temperatures as low as 150°C without incorporating Ge atoms. The epi-Si films were structurally examined using high-resolution x-ray diffraction (HR-XRD) with wavelength of 1.54056 Å, triple-axis x-ray reciprocal-space mapping (RSM), transmission electron microscopy (TEM), and secondary-ion mass spectrometry (SIMS). Additionally, heavily phosphorus-doped (P-doped) epi-Si layers were grown using phosphine ( $\text{PH}_3$ ) doping gas at 150°C.

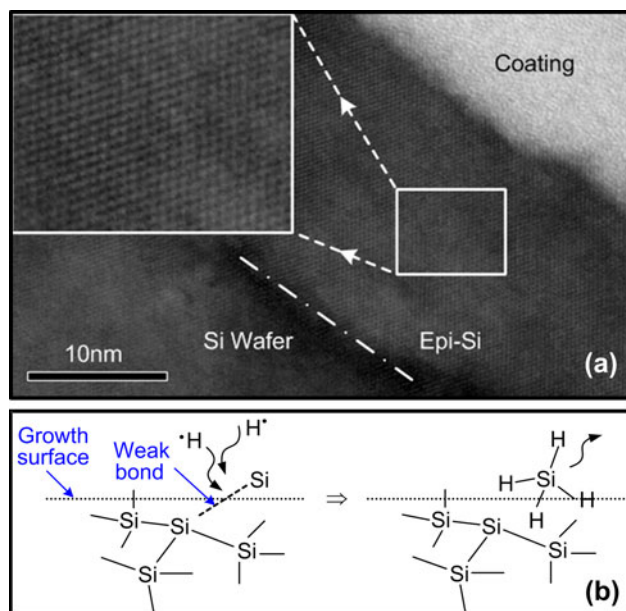


Fig. 1. (a) Representative cross-sectional TEM image of a sample with HDR of 10, showing a well-ordered crystalline structure. (b) Schematic illustration representing the growth mechanism for LTE of Si by PECVD.

The experiments were performed on (100) *p*-type Si substrates. The samples were cleaned using standard piranha solution, followed by dilute HF dip (100:1) for 3 min to remove the native oxide. The samples were then immediately loaded in a PECVD reactor. Undoped silicon films were grown to thickness of 40 nm to 50 nm at 150°C from a mixture of silane ( $\text{SiH}_4$ ) and hydrogen ( $\text{H}_2$ ) at different HDRs, ranging from 7 to 10 with standard 13.56-MHz radiofrequency (RF) plasma. Figure 1a shows cross-sectional TEM images of a sample grown with HDR of 10, exhibiting a well-ordered crystalline structure. The role of hydrogen dilution can be explained within the context of Fig. 1b. We surmise that hydrogen radicals *in situ* remove weak Si-Si bonds from the growth surface, which would otherwise result in growth of a noncrystalline film. As a result, this mechanism will leave strong Si-Si bonds on the growth surface, allowing epitaxial growth of Si to take place if a single-crystalline substrate is used. However, in the absence of a crystalline substrate seed, random nucleation will lead to growth of a nano/microcrystalline layer.<sup>9–11</sup> Furthermore, our data suggest that higher HDR results in reduced epitaxial growth rates. This observation is similar to the effect of hydrogen dilution on the growth rate of a-Si:H, nanocrystalline Si, or microcrystalline Si.

HR-XRD measurements were performed (Fig. 2) to further investigate the structural properties of the samples grown at different HDRs. It is clear from the rocking-curve measurements that the epi-Si layers are compressively strained. The well-defined pendellösung fringes suggest high crystalline quality of the epi-Si films. It is interesting to

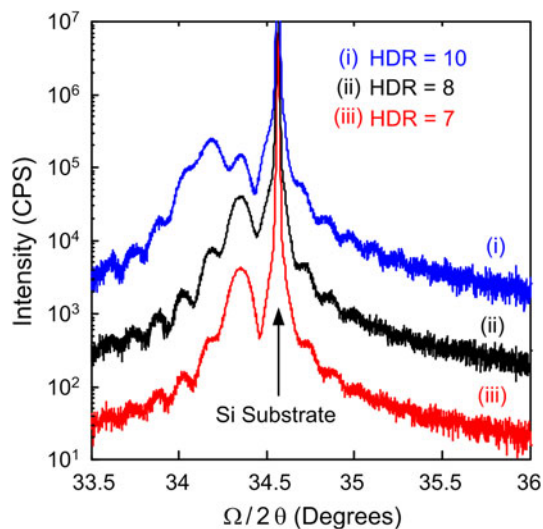


Fig. 2. Measured rocking curves for samples with different HDRs, indicating the growth of compressively strained Si.

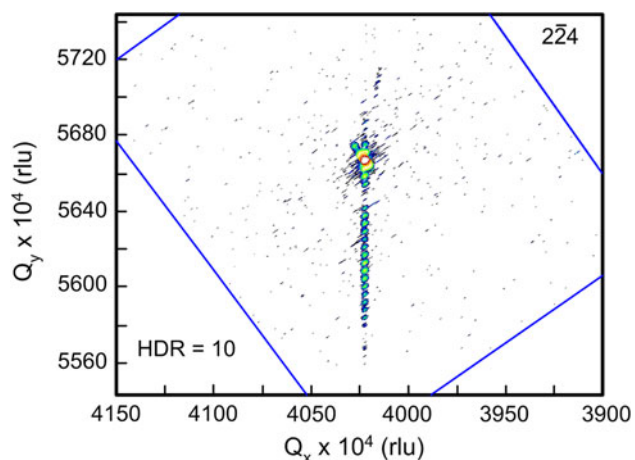


Fig. 3. Representative RSM data for a sample with HDR of 10, indicating that the epi-Si layer is fully strained while the strain is graded.

note that simulation of the rocking-curve data with a reasonable fit was only possible by constructing a multilayer model to emulate a strain gradient. Therefore, to obtain more detailed information about the in-plane and out-of-plane lattice parameters, RSM was performed around the 224 diffraction peak for these samples. Figure 3 shows representative RSM data for the sample with HDR of 10. The vertical streak below the main Si substrate peak in the RSM data is from the epitaxial Si layer. The in-plane lattice component ( $Q_x$ ) shows very little dispersion and is aligned with the main substrate peak. This indicates that the epitaxial layer is pseudomorphic with the substrate, and there is no measurable strain relaxation. The large dispersion in the perpendicular lattice component ( $Q_y$ )

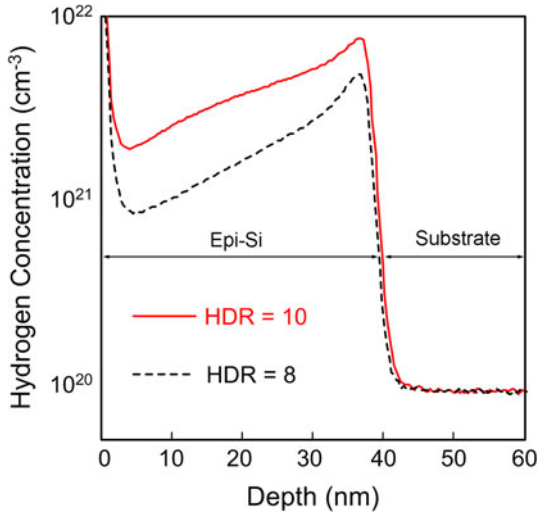


Fig. 4. Hydrogen depth profiles of samples with HDR of 8 and 10.

indicates that there is a distribution of lattice spacings in the  $\langle 001 \rangle$  direction. Furthermore, the equilibrium lattice parameters were determined from the analysis of 004 and 224 diffraction data (mean peak positions) to be 0.5447 nm ( $\epsilon_{xx} = 0.29\%$ ) for the samples with HDR of 7 and 8, and 0.5460 nm ( $\epsilon_{xx} = 0.53\%$ ) for the sample with HDR of 10. For comparison, the deduced strain levels of 0.29% and 0.53% are equivalent in strain to roughly 8 at.% and 14 at.% Ge in SiGe, respectively. The origin of the compressive strain in our low-temperature epi-Si is attributed to the incorporation of hydrogen atoms during the epitaxial growth of Si by PECVD. SIMS measurements were performed on the samples with HDR of 8 and 10 to determine the hydrogen depth profile within the epi-Si layers (Fig. 4). The SIMS data show a graded hydrogen concentration within the epi-Si films, with the greatest concentration occurring at the epi-Si/c-Si substrate. The SIMS depth profile of hydrogen is consistent with the x-ray RSM results, indicating a strain gradient in the epi-Si layers. It is therefore reasonable to deduce that the highest strain occurs in the vicinity of the epi-Si/c-Si substrate interface, where the hydrogen concentration peaks. Furthermore, the SIMS data substantiate that the higher strain level of the sample with HDR of 10 stems from the greater incorporation of hydrogen atoms. To examine the thermal stability of the compressively strained epi-Si layers, a sample with HDR of 10 was consecutively annealed at 100°C, 250°C, 350°C, and 450°C for 30 min in  $N_2$  ambient. Figure 5 illustrates the XRD data measured after each annealing step, indicating the onset of strain reduction in the epi-Si layer at  $\sim 350^\circ\text{C}$ . Furthermore, the reduction of the strain level upon annealing can be attributed to hydrogen escape from the epi-Si layer.

We additionally examined the epitaxy of heavily doped Si at various phosphine ( $\text{PH}_3$ ) doping gas ratios. The P-doped Si films were grown on  $p$ -type

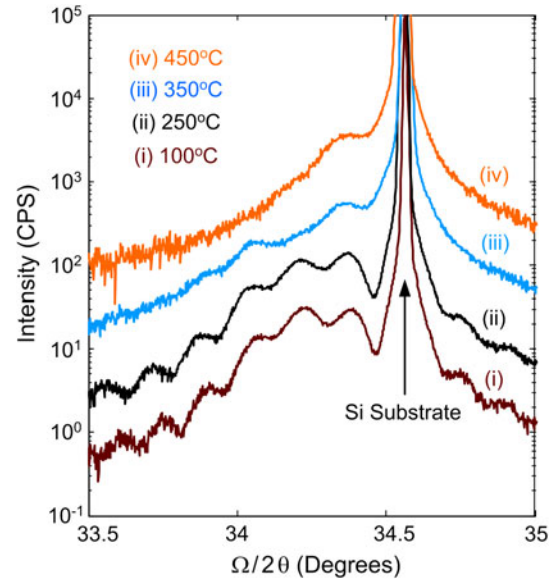


Fig. 5. Rocking-curve data for a sample with HDR of 10 measured after consecutive anneals at 100°C, 250°C, 350°C, and 450°C.

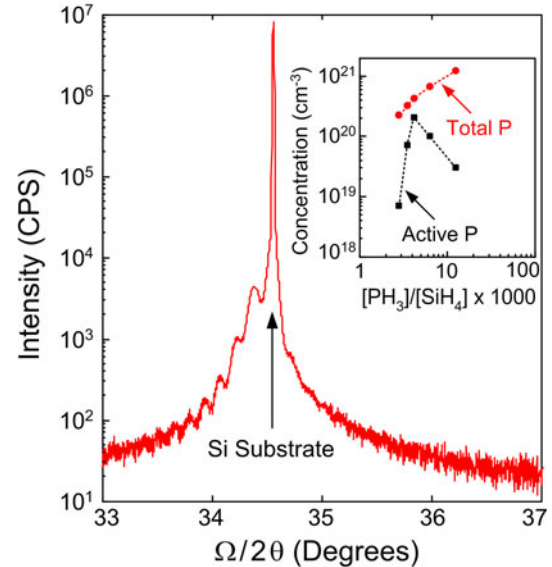


Fig. 6. HR-XRD data for the sample with active P concentration of  $2 \times 10^{20} \text{ cm}^{-3}$ . The inset illustrates the active and total P concentrations for various phosphine-to-silane gas ratios.

(001) Si at HDR of 10. The electrically active doping concentration was estimated from the resistivity of the films,<sup>12</sup> measured by the four-point probe technique. Furthermore, the total concentration of phosphorus impurities was measured by SIMS, showing uniform distribution of phosphorus impurities within the epitaxial layers. The inset in Fig. 6 illustrates the extracted active and total phosphorus concentrations for a range of phosphine/silane gas ratios. It is shown that an active doping concentration as high as  $\sim 2 \times 10^{20} \text{ cm}^{-3}$  can be obtained at

150°C. However, it was observed that further increase of the phosphine/silane gas ratio gave rise to degradation of the conductivity of the P-doped epi-Si and therefore reduction of the active doping concentration. This is conceivably due to surface poisoning by phosphorus adatoms, which is known to disrupt epitaxial growth.<sup>13</sup> The change from crystalline growth to noncrystalline growth at high doping gas flows was confirmed by cross-sectional TEM studies (not shown). It is also notable that the HR-XRD data for P-doped samples reveal a  $\sim 2\times$  reduction in the strain level compared with the undoped samples. Figure 6 illustrates the corresponding HR-XRD data for the sample with the maximum active doping concentration, showing a strain level of  $\sim 0.23\%$ . This shift in strain is too large to be explained by the expected lattice contraction by P incorporation.<sup>14</sup> We speculate that the strain reduction may in part be related to competition between silane and phosphine for adsorption sites on the silicon surface, due to the higher sticking coefficient of P-containing species at lower temperatures.<sup>13</sup>

## CONCLUSIONS

We have demonstrated epitaxy of compressively strained Si at temperatures as low as 150°C using PECVD. The compressive strain in the epi-Si stems from the incorporation of hydrogen during the Si epitaxy. The effect of various hydrogen dilution ratios on the residual compressive lattice strain during the epitaxy of Si was examined using x-ray techniques and SIMS analysis. Additionally, it was shown that highly conductive *n*-epi Si with carrier concentration  $> 2 \times 10^{20} \text{ cm}^{-3}$  can be achieved by phosphine doping at these low temperatures.

## ACKNOWLEDGEMENTS

The authors would like to gratefully thank Dr. Ghavam G. Shahidi for his technical guidance and managerial support, and Professor Sigurd Wagner of Princeton University for stimulating scientific discussions and allowing use of his PECVD facility for this work.

## REFERENCES

1. D.J. Eaglesham, F.C. Unterwald, H. Luftman, D.P. Adams, and S.M. Yalisove, *J. Appl. Phys.* 74, 6615 (1993).
2. K. Baert, P. Deschepper, J. Poortmans, J. Nijs, and R. Mertens, *Appl. Phys. Lett.* 60, 442 (1992).
3. T. Kitagawa, M. Kondo, and A. Matsuda, *Appl. Surf. Sci.* 159–160, 30 (2000).
4. M.F. Baroughi, H.G. El-Gohary, C.Y. Cheng, and S. Sivoththaman, *Mater. Res. Soc. Symp. Proc.* 989, 19 (2007).
5. J. Damon-Lacoste and P. Roca i Cabarrocas, *J. Appl. Phys. Lett.* 105, 063712 (2009).
6. M.L. Lee, E.A. Fitzgerald, M.T. Bulsara, M.T. Currie, and A. Lochtefeld, *J. Appl. Phys.* 97, 011101 (2005).
7. T. Ghani, M. Armstrong, C. Auth, M. Bost, P. Charvat, G. Glass, T. Hoffmann, K. Johnson, C. Kenyon, J. Klaus, B. McIntyre, K. Mistry, A. Murthy, J. Sandford, M. Silberstein, S. Sivakumar, P. Smith, K. Zawadzki, S. Thompson, and M. Bohr, *IEDM Tech. Dig.*, 978 (2003).
8. Z. Lou, Y.F. Chong, J. Kim, N. Rovedo, B. Greene, S. Panda, T. Sato, J. Holt, D. Chidambarao, J. Li, R. Davis, A. Madan, A. Turansky, O. Gluschenkov, R. Lindsay, A. Ajmera, J. Lee, S. Mishra, R. Amos, D. Schepis, H. Ng, and K. Rim, *IEDM Tech. Dig.*, 489 (2005).
9. J. Koh, A.S. Ferlauto, P.I. Rovira, C.R. Wronski, and R.W. Collins, *Appl. Phys. Lett.* 75, 2286 (1999).
10. P. Roca i Cabarrocas, N. Layadi, T. Heitz, B. Drevillon, and I. Solomon, *Appl. Phys. Lett.* 66, 3609 (1995).
11. A.S. Ferlauto, R.J. Koval, C.R. Wronski, and R.W. Collins, *Appl. Phys. Lett.* 80, 2666 (2002).
12. W.E. Beadle, J.C. Tsai, and R.D. Plummer, *Quick Reference to Manual for Silicon Integrated Circuit Technology* (New York: Wiley, 1985).
13. B.S. Meyerson and M.L. Yu, *J. Electrochem. Soc.* 131, 2366 (1984).
14. K.G. McQuhae and A.S. Brown, *Solid State Electron.* 15, 259 (1972).